AN INVESTIGATION OF 3D HEAT AND MASS TRANSFER IN MAGNETOHYDRODYNAMICS LAMINAR FLOW ABOUT AN INCLINED SEMI-INFINITE POROUS PLATE

LINAH MOGIRANGO ONYINKWA

I56/CE/ 34148 / 2016

A Project Submitted in Partial Fulfilment of the Requirement for the Award of the Degree of Master of Science in Applied Sciences of Kenyatta University.

March 2022

Declaration

This study is my original work and has not been presented for a degree in any other University

Signature …… Date ……..

LINAH M. ONYINKWA

I56/CE/ 34148 / 2016

This study has been submitted for examination with our approval as the University Supervisor.

Signature ……. Date ……

DR. CHEPKWONY

DEPARTMENT OF MATHEMATICS

KU- KENYA

Abstract

Investigation of transmission of mass and heat in magnetohydrodynamics (MHD) flow over a plate inclined at an angle past semi-infinite porous plate is carried out in this study. MHD flow model is formulated by combining the electromagnetic laws with Navier-stokes equations. The equations that govern the flow are transformed into their dimensionless form. The numerical scheme in the form of Implicit finite centre difference is used to obtain a numerical solution to the equations in MATLAB. The numerical results are presented graphically by varying the parameters that emerged from the flow. Effects of porosity parameter, magnetic strength parameter, and the inclination angle are studied. Velocity profiles in all directions are reduced with increasing porosity, magnetic field and inclination angle while there is a raise in the temperature profiles with increasing porosity, magnetic field and surface inclination angle.

NOMENCLATURE

Symbols	Meaning
u, v, w	Dimensional velocities in the x, y, z directions
T	Dimensional temperature
C	Dimensional concentration
$T_w\ (T_\infty)$	Temperature of the wall (free stream)
$C_w,\ C_\infty$	Concentration of the wall and free stream respectively
B_0	Magnetic field strength
K_0	Porosity
D_B	Brownian coefficient
D_T	Thermophoretic coefficient
η	Similarity variable
β, β^*	Coefficient thermal and solutal expansivity
g^*	Acceleration due to gravity
α	Inclination angle
ρ	Density of fluid
c_p	Heat capacity of the fluid
σ	Electrical conductivity
μ	Dynamic viscosity
ν	Kinematic viscosity
$Gr_t^1,\ Gr_t^2$	Thermal Grashof number in the x- and y- directions respectively
$Gr_s^1,\ Gr_s^2$	Solutal Grashof number in the x- and y- directions respectively
M	Magnetic field parameter
k	Thermal diffusivity
k_*	Porosity parameter
Sc	Schmidt number
$N_b,\ N_t$	Brownian and thermophoretic parameters
HMT	Heat and Mass Transfer
MF	Magnetic field

Table of Contents

CHAPTER 1

INTRODUCTION

1.1 Background Information

A force tends to move a conduit carrying a flow of electricity perpendicular to the electric field when it moves in a magnetic field. When a conductor travels in a MF, a current is generated along the perpendicular direction to the field and the motion directions. These findings were initially made by Michael Faraday in 1831, and they are now known as electromagnetic laws. The fundamentals of motor and dynamo functioning are defined by these laws. Fluids have the capacity to conduct electricity in a MF in general and the flow induces a current in which mechanical forces are exerted. Such fluids include liquid metals, salt water and plasma. Due to the MF generated by the induced current, the original MF changes. This two-way inter-action produces the Lorentz force. The equations governing MHD flow comprise the momentum equation and Maxwell's equation of electromagnetism.

Heat and mass transfer has applications in science and technology such as in the functions of devices and systems, heat engine, thermal diode and thermoelectric warmer. Moreover, heat exchanger is an application of heat transfer which is commonly used in refrigeration and chemical processing. Mass transfer takes place in various processes such as membrane filtration and adsorption. Scholars' attentions have not been drawn to the flow in three-dimensional frame where the flow happens across a tilted surface so that the flow is uphill. This study attempts to unravel such flow in a 3D frame.

1.2 Problem Statement

Researches done on MHD fluid flow (Ostratch 1972, Nyabuto, et. al 2017) investigated properties of the fluid in 2-Dimensional fluid flow which may not satisfactorily describe the flow in the physical systems. This research seeks to investigate 3-Dimensional fluid flow over a porous plate tilted at an angle to the fluid flow that is applicable to bulk system. The study of MHD flow on an inclined porous surface is quite vital as it will shed more light on the fluid and has applications in plasma studies, petroleum industries and engineering.

1.3 Objectives

1.4 General Objective

To analyse heat and mass transfer effects on MHD flow about a plate inclined at an angle past a semi-infinite porous plate.

1.5 Specific Objectives

To determine;

(i) The MF effects on mass transfer in MHD flow about a plate inclined at an angle past semi-infinite porous plate.

(ii) The MF effects on heat transfer in MHD flow about a plate inclined at an angle past semi-infinite porous plate.

(iii) The MF effects on skin friction of an MHD flow about a plate inclined at an angle past semi-infinite porous plate.

1.6 Justification

MHD flow on an inclined porous surface is applied in MHD generators and flow meters. The knowledge is applied in meeting societal needs as it is used in mineral exploration which gives the miners income. Study of plasma confinement will help mankind to remove energy shortage which is a major problem in the human society. Furthermore, because MHD energy generation is pollution-free, it will considerably reduce environmental pollution. Because of its wide applicability in research and technology, understanding HMT in MHD is essential.

1.7 Definition of Terms

Magnetohydrodynamics (MHD) (Oke et al., 2022)

It refers to the study of fluids that possess the capacity to conduct electricity in a MF. The term magnetohydrodynamics is derived from; magneto (referring to MF); hydro (referring to fluids); and dynamics (referring to motion).

Fluid (Oke et al., 2020)

Substances that get deformed repeatedly under any size of shear stress applied. It consists of both liquids and gases.

Viscous flow (Juma et al., 2022a)

Viscosity measures the flowing fluid's resistance to shear. It causes friction as the fluid flows. This brings about friction in the flow.

Mass transfer (Juma et al., 2022b)

This is the net mass movement from point 1 to point 2. It takes place due to concentration gradient. Mass transfer occurs in the processes such as evaporation, filtration, drying, precipitation, distillation and absorption.

Heat transfer (Juma et al., 2022a)

The difference in temperature between boundaries and ambient fluid gives rise to temperature variations in the fluid. Heat transfer refers to energy transfer that occurs between material bodies due to temperature difference. The temperature difference is as a result of absorption of thermal radiation, radioactivity and discharge of latent heat as the fluid vapour condenses. Heat transmits via solid through conduction, via liquid through convection and via vacuum through radiation.

Incompressible flow (Animasaun et al., 2023)

This is when density of a fluid flows is invariant with time.

CHAPTER 2

LITERATURE REVIEW

Most researches in MHD are attributed to Hannes Alfven (1908-1995), who predicted that the earth's MF would cause induced currents in the ocean. Since then, several analytical studies have been done by various scholars in MHD leading to various applications such as various forms of heat generation that are discussed in natural convection phenomena. This is seen, for example in the formulation of the boundary value problem that describes the convection phenomena, and in this Hannes assumed that the motion is 2D and steady and that the fluid is incompressible and friction that results on heating is negligible. Nyabuto *et al*., 2015 investigated MHD stokes-free convection of an incompressible fluid on a vertical porous semi-infinite plate. They applied a uniform MF perpendicular to the flow. They found that raising Hartmann causes a decrease in velocity profile. This proposed research considers a three-dimensional fluid flow system under applied magnet field. Katagiri *et. al* (2011) studied MHD incompressible Couette flow induced by spontaneously moving plate. Rao *et al*., (2012) investigated MHD free convective HMT flow past a linearly accelerated vertical porous plate. They found out that magnetic parameter, Schmidt number and Grashof number are directly proportional to the skin friction. Oke (2020a,b) explores the impact of the Coriolis force on the motion of air over the uhspr and observed that the Coriolis force has a significant impact on the motion of air over the uhspr, and this finding has implications for understanding atmospheric dynamics.

Onyango *et al*. (2015) took into consideration injection and suction in MHD flow between two parallel porous plate. The velocity profile increases with increasing pressure gradient. Reddy and Murthy (2011) investigated MHD flow with viscous dissipation, double-diffusive convection and chemical reaction. He observed a relationship between Prandtl number, temperature and velocity.

Increase in Schmidt number causes decrease in velocity profile and decrease in Schmidt number leads to increase in concentration.

Mburu Mbugua (2016) studied MHD flow between two parallel porous plates in which one is moving. They established that temperature profile is directly proportional to suction parameter and velocity is inversely proportional to the suction parameter. Beg *et al*. (2009) investigated Hall current on unsteady MHD Hartmann-Couette flow. Singh *et al*. (2015) investigated MHD flow within a channel in which one plate is moving. Hayat *et al*. (2017) studied cross diffusion effects on forced convection heat transfer boundary layer flow of an elastic-viscous fluids along a stretched perpendicular surface in a porous boundary. Umamaheswar *et al*. (2016) investigated viscous dissipation on MHD flow of viscoelastic fluid past an inclined permeable plate. Hamad et al. (2019) investigated time dependent MHD natural convection flow through a vertical permeable flat plate for a nano-fluid with unvarying heat generation. Ali et al. (2013) studied thermal radiation influence on free convective flow along a vertical surface in a medium of gray gas. Sundarammal and Naisha (2019) paid attention to MHD squeeze film characteristics between porous parallel plates with effect of surface roughness.

In this study, HMT in MHD about a plate inclined at an angle past semi-infinite porous medium is investigated.

CHAPTER 3

METHODOLOGY

3.1 Formulation of Governing Equations

The laminar incompressible viscous flow considered in this study is a three-dimensional flow across an inclined porous plate with constant magnetic field. The flow is taken in a magnetic field (MF) with constant MF strength. Assumptions of the model are;

(a) The fluid flow is incompressible steady.

(b) The concentration of foreign mass is low hence Dufour and Soret effects can be ignored.

(c) The plate is at rest and it is a non-conductor

(d) The hall current is too small and there is no applied or polarization voltage.

(e) MF applied orthogonal to the plate is and induced MF is negligible.

The x-axis is taken horizontally parallel to the plate along the flow, y axis is perpendicular to the semi-infinite porous plate. The MF strength that is applied perpendicularly to the semi- infinite porous plate has uniform strength B_0. The fluid layer next to the surface is considered to take the surface properties to ascertain that the no-slip condition is maintained. The surface stretches linearly at the rate ax and the correction factor $\cos\alpha$ is included in the corresponding terms to pay for the inclination of the surface. The model consists of the continuity, momentum, energy and mass concentration equations. The physical configuration of the flow is shown in Figure 3.1.

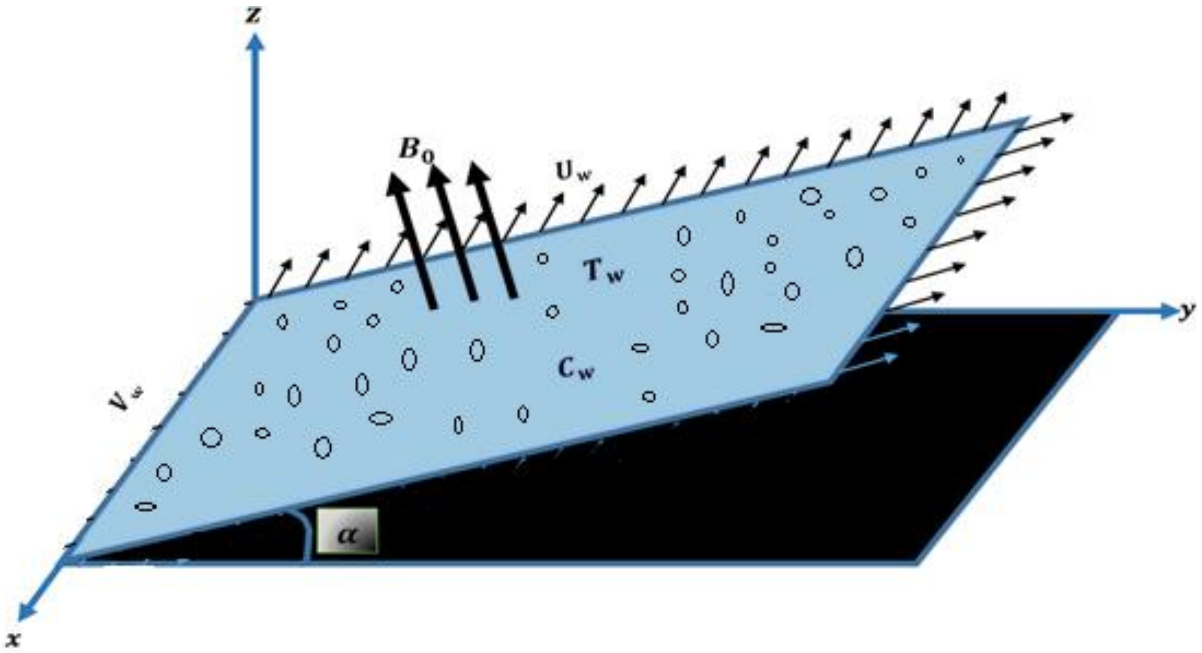

Figure 3.1: Flow configuration

The boundary layer equations obtained from the Navier Stokes' equations are given as the system of five Partial Difference Equations (PDEs) consisting of one continuity equation, two momentum equations (because the flow is three-dimensional), one energy equation and one species equation. The system is as follows;

$$\begin{cases} \nabla \cdot \underline{U} = 0 & (3.1a) \\ u\dfrac{\partial u}{\partial x} + \mathrm{v}\dfrac{\partial u}{\partial y} + w\dfrac{\partial u}{\partial z} = \nu\dfrac{\partial^2 u}{\partial z^2} + g^*\big(\beta(T-T_\infty) + \beta^*(C-C_\infty)\big)\cos\alpha - \dfrac{\sigma B_0^2\cos\alpha}{\rho}u - \dfrac{\nu}{K_0}u & (3.1b) \\ u\dfrac{\partial \mathrm{v}}{\partial x} + \mathrm{v}\dfrac{\partial \mathrm{v}}{\partial y} + w\dfrac{\partial \mathrm{v}}{\partial z} = \nu\dfrac{\partial^2 \mathrm{v}}{\partial z^2} + g^*\big(\beta(T-T_\infty) + \beta^*(C-C_\infty)\big)\cos\alpha + \dfrac{\sigma B_0^2\cos\alpha}{\rho}\mathrm{v} - \dfrac{\nu}{K_0}\mathrm{v} & (3.1c) \\ u\dfrac{\partial T}{\partial x} + \mathrm{v}\dfrac{\partial T}{\partial y} + w\dfrac{\partial T}{\partial z} = \dfrac{k}{\rho c_p}\dfrac{\partial^2 T}{\partial z^2} + \tau\left(\dfrac{D_B}{\Delta C}\dfrac{\partial C}{\partial z}\dfrac{\partial T}{\partial z} + \dfrac{D_T}{T_\infty}\left(\dfrac{\partial T}{\partial z}\right)^2\right) & (3.1d) \\ u\dfrac{\partial C}{\partial x} + \mathrm{v}\dfrac{\partial C}{\partial y} + w\dfrac{\partial C}{\partial z} = D_B\dfrac{\partial^2 C}{\partial z^2} + \dfrac{D_T\Delta C}{T_\infty}\dfrac{\partial^2 T}{\partial z^2} & (3.1e) \end{cases}$$

where $\underline{U} = (u, v, w)$ and subject to the boundary layer and free stream conditions;

$$\begin{cases} u = ax, \ \mathrm{v} = ay, \quad w = 0, \ T = T_w, \ C = C_w & \text{at } z = 0 \qquad (3.2a) \\ u \to 0, \quad v \to 0, \quad T \to T_\infty, \quad C \to C_\infty & \text{as } z \to \infty \qquad (3.2b) \end{cases}$$

3.2 Similarity Transformation

The first step in solving system (3.1) with the condition (3.2) is the reduction of the system to its dimensionless form. This process requires the use of the Similarity variables

$$\begin{cases} \eta = z\left(\frac{a}{\mathrm{v}}\right)^{\frac{1}{2}}, \ \Theta = \frac{T - T_\infty}{T_w - T_\infty}, \ \Phi = \frac{C - C_\infty}{C_w - C_\infty}, \\ u = axf', \ v = ayg', \qquad w = -(av)^{\frac{1}{2}}(f + g). \end{cases} \qquad (3.3)$$

Now, from the similarity variable $\eta = z\left(\frac{a}{\mathrm{v}}\right)^{1/2}$, we have that

$$\frac{\partial \eta}{\partial x} = \frac{\partial \eta}{\partial y} = 0, \quad \frac{\partial \eta}{\partial z} = \left(\frac{a}{\mathrm{v}}\right)^{\frac{1}{2}}. \qquad (3.4)$$

From here, finding the partial derivatives of $u = axf'$, $v = ayg'$ and $w = -(av)^{\frac{1}{2}}(f + g)$ gives the following;

$$\begin{cases} \frac{\partial u}{\partial x} = af', \ \frac{\partial u}{\partial y} = 0, \ \frac{\partial u}{\partial z} = \frac{\partial u}{\partial \eta}\frac{\partial \eta}{\partial z} = \left(\frac{a}{\mathrm{v}}\right)^{\frac{1}{2}} axf'', \ \frac{\partial^2 u}{\partial z^2} = \frac{\partial}{\partial \eta}\left(\frac{\partial u}{\partial \eta}\right)\frac{\partial \eta}{\partial z} = \frac{a^2 x}{\nu} f''', \\ \frac{\partial \mathrm{v}}{\partial x} = 0, \ \frac{\partial \mathrm{v}}{\partial y} = ag', \ \frac{\partial \mathrm{v}}{\partial z} = \frac{\partial \mathrm{v}}{\partial \eta}\frac{\partial \eta}{\partial z} = \left(\frac{a}{\mathrm{v}}\right)^{\frac{1}{2}} ayg'', \ \frac{\partial^2 \mathrm{v}}{\partial z^2} = \frac{\partial}{\partial \eta}\left(\frac{\partial \mathrm{v}}{\partial \eta}\right)\frac{\partial \eta}{\partial z} = \frac{a^2 y}{\nu} g''', \\ \frac{\partial w}{\partial x} = 0, \ \frac{\partial w}{\partial y} = 0, \ \frac{\partial w}{\partial z} = \frac{\partial w}{\partial \eta}\frac{\partial \eta}{\partial z} = -\left(\frac{a}{\mathrm{v}}\right)^{\frac{1}{2}} \frac{\partial}{\partial \eta}\left((av)^{\frac{1}{2}}(f + g)\right) = -a(f' + g'). \end{cases} \qquad (3.5)$$

The continuity equation (3.1a)

$$\nabla \cdot \underline{U} = 0$$

is therefore satisfied. Now, we consider the first momentum equation (3.1b)

$$u\frac{\partial u}{\partial x}+\mathrm{v}\frac{\partial u}{\partial y}+w\frac{\partial u}{\partial z}=\nu\frac{\partial^2 u}{\partial z^2}+g^*\big(\beta(T-T_\infty)+\beta^*(C-C_\infty)\big)\cos\alpha-\frac{\sigma B_0^2\cos\alpha}{\rho}u-\frac{\nu}{K_0}u.$$

So that

$$(axf')(af')+(ayg')(0)-(a\nu)^{\frac{1}{2}}(f+g)\left(\frac{a}{\nu}\right)^{\frac{1}{2}}axf''$$

$$=\nu\frac{a^2x}{\nu}f'''+g^*(\beta(T_w-T_\infty)\Theta+\beta^*(C_w-C_\infty)\Phi)\cos\alpha-\frac{\sigma B_0^2\cos\alpha}{\rho}axf'-\frac{\nu}{K_0}axf'$$

$$a^2x((f')^2-(f+g)f'')$$

$$=a^2xf'''+g^*(\beta(T_w-T_\infty)\Theta+\beta^*(C_w-C_\infty)\Phi)\cos\alpha-\frac{\sigma B_0^2\cos\alpha}{\rho}axf'-\frac{\nu}{K_0}axf'$$

$$f'''-(f')^2+(f+g)f''$$

$$+\left(\frac{g^*\beta(T_w-T_\infty)}{a^2x}\Theta+\frac{g^*\beta^*(C_w-C_\infty)}{a^2x}\Phi-\frac{\sigma B_0^2}{a\rho}f'\right)\cos\alpha-\frac{\nu}{aK_0}f'=0.$$

By setting the parameters

$$Gr_t^1=\frac{g^*\beta(T_w-T_\infty)}{a^2x},\quad Gr_s^1=\frac{g^*\beta^*(C_w-C_\infty)}{a^2x},\quad M=\frac{\sigma B_0^2}{a\rho},\quad k_*=\frac{\nu}{aK_0}$$

The equation becomes

$$f'''-(f')^2+(f+g)f''+(Gr_t^1\Theta+Gr_s^1\Phi-Mf')\cos\alpha-k_*f'=0.$$

Next is to consider the second momentum equation (3.1c)

$$u\frac{\partial \mathrm{v}}{\partial x}+\mathrm{v}\frac{\partial \mathrm{v}}{\partial y}+w\frac{\partial \mathrm{v}}{\partial z}=\nu\frac{\partial^2 \mathrm{v}}{\partial z^2}+g^*\big(\beta(T-T_\infty)+\beta^*(C-C_\infty)\big)\cos\alpha+\frac{\sigma B_0^2\cos\alpha}{\rho}\mathrm{v}-\frac{\nu}{K_0}\mathrm{v}.$$

So that

$$(axf')(0) + (ayg')(ag') - (av)^{\frac{1}{2}}(f+g)\left(\frac{a}{\nu}\right)^{\frac{1}{2}} ayg''$$

$$= \nu\frac{a^2y}{\nu}g''' + g^*(\beta(T_w - T_\infty)\Theta + \beta^*(C_w - C_\infty)\Phi)\cos\alpha - \frac{\sigma B_0^2\cos\alpha}{\rho}ayg' - \frac{\nu}{K_0}ayg'$$

$$a^2y((g')^2 - (f+g)g'')$$

$$= a^2yg''' + g^*(\beta(T_w - T_\infty)\Theta + \beta^*(C_w - C_\infty)\Phi)\cos\alpha - \frac{\sigma B_0^2\cos\alpha}{\rho}ayg' - \frac{\nu}{K_0}ayg'$$

$$g''' - (g')^2 + (f+g)g''$$

$$+\left(\frac{g^*\beta(T_w - T_\infty)}{a^2y}\Theta + \frac{g^*\beta^*(C_w - C_\infty)}{a^2y}\Phi - \frac{\sigma B_0^2}{a\rho}g'\right)\cos\alpha - \frac{\nu}{aK_0}g' = 0.$$

and setting the parameters

$$Gr_t^2 = \frac{g^*\beta(T_w - T_\infty)}{a^2y},\ \ Gr_s^2 = \frac{g^*\beta^*(C_w - C_\infty)}{a^2y},$$

we have the dimensionless form as

$$g''' - (g')^2 + (f+g)g'' + (Gr_t^2\Theta + Gr_s^2\Phi - Mg')\cos\alpha - k_*g' = 0.$$

Next is the energy equation (3.1d)

$$u\frac{\partial T}{\partial x} + \mathrm{v}\frac{\partial T}{\partial y} + w\frac{\partial T}{\partial z} = \frac{k}{\rho c_p}\frac{\partial^2 T}{\partial z^2} + \tau\left(\frac{D_B}{\Delta C}\frac{\partial C}{\partial z}\frac{\partial T}{\partial z} + \frac{D_T}{T_\infty}\left(\frac{\partial T}{\partial z}\right)^2\right).$$

Consider the derivatives of T and C, where

$$T = T_\infty + (T_w - T_\infty)\Theta, \quad C = C_\infty + (C_w - C_\infty)\Phi,$$

then

$$\frac{\partial T}{\partial x}=0,\quad \frac{\partial T}{\partial y}=0,\quad \frac{\partial T}{\partial z}=\frac{\partial T}{\partial \eta}\frac{\partial \eta}{\partial z}=\left(\frac{a}{\nu}\right)^{\frac{1}{2}}(T_w-T_\infty)\Theta',\quad \frac{\partial^2 T}{\partial z^2}=\frac{a(T_w-T_\infty)}{\nu}\Theta'',$$

$$\frac{\partial C}{\partial x}=0,\quad \frac{\partial C}{\partial y}=0,\quad \frac{\partial C}{\partial z}=\frac{\partial C}{\partial \eta}\frac{\partial \eta}{\partial z}=\left(\frac{a}{\nu}\right)^{\frac{1}{2}}(C_w-C_\infty)\Phi',\quad \frac{\partial^2 T}{\partial z^2}=\frac{a(C_w-C_\infty)}{\nu}\Phi''.$$

So that the energy equation (3.1d) becomes

$$(axf')(0)+(ayg')(0)-(a\nu)^{\frac{1}{2}}(f+g)\left(\frac{a}{\nu}\right)^{\frac{1}{2}}(T_w-T_\infty)\Theta'=\frac{k}{\rho c_p}\frac{a(T_w-T_\infty)}{\nu}\Theta''$$

$$+\tau\left(\frac{D_B}{\Delta C}\left(\frac{a}{\nu}\right)^{\frac{1}{2}}(C_w-C_\infty)\Phi'\left(\frac{a}{\nu}\right)^{\frac{1}{2}}(T_w-T_\infty)\Theta'+\frac{D_T}{T_\infty}\left(\left(\frac{a}{\nu}\right)^{\frac{1}{2}}(T_w-T_\infty)\Theta'\right)^2\right)$$

$$-a(T_w-T_\infty)(f+g)\Theta'$$

$$=\frac{k}{\rho c_p}\frac{a(T_w-T_\infty)}{\nu}\Theta''+\tau\left(\frac{aD_B}{\nu}(T_w-T_\infty)\Phi'\Theta'+\frac{aD_T}{\nu T_\infty}(T_w-T_\infty)^2(\Theta')^2\right)$$

$$\Theta''+\frac{\nu\rho c_p}{k}(f+g)\Theta'+\frac{\tau D_B\rho c_p}{k}\Phi'\Theta'+\frac{\rho c_p\tau D_T}{kT_\infty}(T_w-T_\infty)(\Theta')^2=0$$

Setting the parameters as

$$Pr=\frac{\nu\rho c_p}{k},\quad N_b=\frac{\tau D_B\rho c_p}{k},\quad N_t=\frac{\rho c_p\tau D_T}{kT_\infty}(T_w-T_\infty)$$

The dimensionless form of the energy equation is therefore

$$\Theta''+Pr(f+g)\Theta'+N_b\Phi'\Theta'+N_t(\Theta')^2=0$$

and next is the species equation (3.1e)

$$u\frac{\partial C}{\partial x}+\mathrm{v}\frac{\partial C}{\partial y}+w\frac{\partial C}{\partial z}=D_B\frac{\partial^2 C}{\partial z^2}+\frac{D_T\Delta C}{T_\infty}\frac{\partial^2 T}{\partial z^2}$$

becomes

$$(axf')(0) + (ayg')(0) - (av)^{\frac{1}{2}}(f+g)\left(\frac{a}{\nu}\right)^{\frac{1}{2}}(C_w - C_\infty)\Phi'$$

$$= \frac{aD_B(C_w - C_\infty)}{\nu}\Phi'' + \frac{D_T\Delta C}{T_\infty}\frac{a(T_w - T_\infty)}{\nu}\Theta''$$

Dividing through by $aD_B(C_w - C_\infty)/\nu$ and rearranging gives

$$\Phi'' + \frac{D_T(T_w - T_\infty)}{T_\infty D_B}\Theta'' + \frac{\nu}{D_B}(f+g)\Phi' = 0.$$

Setting the parameters

$$Sc = \frac{\nu}{D_B}$$

We get the dimensionless form as

$$\Phi'' + \frac{N_t}{N_b}\Theta'' + Sc(f+g)\Phi' = 0.$$

The boundary condition (3.2a) is transformed as follows

At $z = 0$, $\eta = 0$, and

$$u = ax \quad \Rightarrow \quad axf' = ax \quad \Rightarrow \quad f' = 1;$$

$$\mathrm{v} = ax \quad \Rightarrow \quad ayg' = ay \quad \Rightarrow \quad g' = 1;$$

$$w = 0 \quad \Rightarrow \quad -(av)^{\frac{1}{2}}(f+g) = 0 \quad \Rightarrow \quad f+g = 0;$$

$$T = T_w \quad \Rightarrow \quad \Theta = \frac{T_w - T_\infty}{T_w - T_\infty} = 1;$$

$$C = C_w \quad \Rightarrow \quad \Phi = \frac{C_w - C_\infty}{C_w - C_\infty} = 1$$

As $z \to \infty$, $\eta \to \infty$ and

$$u \to 0 \quad \Rightarrow \quad axf' = 0 \quad \Rightarrow \quad f' = 0;$$

$$v \to 0 \quad \Rightarrow \quad ayg' = 0 \quad \Rightarrow \quad g' = 0;$$

$$T = T_\infty \quad \Rightarrow \quad \Theta = \frac{T_\infty - T_\infty}{T_w - T_\infty} = 0;$$

$$C = C_\infty \quad \Rightarrow \quad \Phi = \frac{C_\infty - C_\infty}{C_w - C_\infty} = 0;$$

The dimensionless form of the system of equations (3.1)

$$f''' - (f')^2 + (f+g)f'' + (Gr_t^1\Theta + Gr_s^1\Phi - Mf')\cos\alpha - k_* f' = 0, \qquad (3.6a)$$

$$g''' - (g')^2 + (f+g)g'' + (Gr_t^2\Theta + Gr_s^2\Phi - Mg')\cos\alpha - k_* g' = 0, \qquad (3.6b)$$

$$\Theta'' + Pr(f+g)\Theta' + N_b\Phi'\Theta' + N_t(\Theta')^2 = 0, \qquad (3.6c)$$

$$\Phi'' + \frac{N_t}{N_b}\Theta'' + Sc(f+g)\Phi' = 0. \qquad (3.6d)$$

and the dimensionless form of the boundary conditions (3.2)

$$\begin{cases} at\ \eta = 0; & f' = 1;\ g' = 1;\ f+g = 0;\ \Theta = 1;\ \Phi = 1 \qquad (3.7a) \\ \text{as } \eta \to \infty; & f' = 0;\ g' = 0;\ \Theta = 0;\ \Phi = 0; \qquad (3.7b) \end{cases}$$

where

$$\begin{cases} Gr_t^1 = \dfrac{g^*\beta(T_w - T_\infty)}{a^2 x}, \quad Gr_s^1 = \dfrac{g^*\beta^*(C_w - C_\infty)}{a^2 x}, \quad M = \dfrac{\sigma B_0^2}{a\rho}, & (3.8a) \\ k_* = \dfrac{\nu}{aK_0}, \ Sc = \dfrac{\nu}{D_B}, \ Gr_t^2 = \dfrac{g^*\beta(T_w - T_\infty)}{a^2 y}, \ Gr_s^2 = \dfrac{g^*\beta^*(C_w - C_\infty)}{a^2 y}, & (3.8b) \\ Pr = \dfrac{\nu\rho c_p}{k}, \quad N_b = \dfrac{\tau D_B \rho c_p}{k}, \quad N_t = \dfrac{\rho c_p \tau D_T}{kT_\infty}(T_w - T_\infty) & (3.8c) \end{cases}$$

3.3 Numerical Method

The dimensionless form (3.6) and (3.8) are converted to a system of first order ordinary differential equations by setting

$$x_1 = f, \quad x_2 = f', \quad x_3 = f'', \quad x_4 = g, \quad x_5 = g',$$
$$x_6 = g'', \quad x_7 = \Theta, \quad x_8 = \Theta', \quad x_9 = \Phi, \quad x_{10} = \Phi',$$

and we have

$$\begin{cases} x_1' = x_2 \\ x_2' = x_3 \\ x_3' = -(-x_2^2 + (x_1 + x_4)x_3 + (Gr_t^1\, x_7 + Gr_s^1\, x_9 - Mx_2)\cos\alpha - k_* x_2), \\ x_4' = x_5 \\ x_5' = x_6 \\ x_6' = -(-x_5^2 + (x_1 + x_4)x_6 + (Gr_t^2 x_7 + Gr_s^2 x_9 - Mx_5)\cos\alpha - k_* x_5) \\ x_7' = x_8 \\ x_8' = -(Pr(x_1 + x_4)x_8 + N_b x_8 x_{10} + N_t x_8^2), \\ x_9' = x_{10} \\ x_{10}'' = -\left(\frac{N_t}{N_b} x_8' + Sc(x_1 + x_4)x_{10}\right) \end{cases} \tag{3.9}$$

with the boundary conditions

$$x_2(0) = 1, \ \ x_5(0) = 1, \ \ x_1(0) + x_4(0) = 0, \quad x_7(0) = 1, \quad x_9(0) = 1, \tag{3.10a}$$

$$x_2(\infty) = 0, \qquad x_5(\infty) = 0, \ \ x_7(0) = 0, \quad x_9(0) = 0. \tag{3.10b}$$

The coefficient of skin friction is given as

$$Re^{\frac{1}{2}} C_f = f''(0),$$

where Re is the Reynold's number. The MATLAB solver bvp4c is adopted to obtain the solution to the system of equations.

CHAPTER 4

Analysis and Discussion of Results

The dimensionless form of the governing system of partial differential equations (3.1) and BCs (3.2) are formulated into a system of ordinary differential equations (ODE) (3.6) and (3.7) respectively. The resulting system (3.6) is further rewritten as a system of first order ODE given in (3.9) with the corresponding boundary conditions (3.10). The Implicit centre difference scheme is used to solve the system of first order ODEs (3.9) numerically and the results are displayed as graphs. The default values of the parameters used are

$$Gr_t^1 = Gr_t^2 = Gr_s^1 = Gr_s^2 = 1,\ \ M = 1,\ \ \ k_* = 1,\ \ Pr = 7,\ \ \ N_b = N_t = 1,\ \ Sc = 1.$$

In what follows, the primary velocity represents the dimensionless velocity in the x-direction and the secondary velocity represents the velocity in the y-direction.

The effects of inclination angle on the magnetohydrodynamic flow about an inclined porous plate are highlighted in figures (4.1) – (4.4). From figures (4.1) and (4.2), both the secondary velocity and the primary velocity are reduced as the inclination angle increases. It is to be noted that the surface is a flat horizontal surface when $\alpha = 0$, inclined surface when $0 < \alpha < \frac{\pi}{2}$ and vertical when $\alpha = \frac{\pi}{2}$. Hence, increasing the inclination angle means that more kinetic energy will be converted to heat energy, hence reducing the velocity in all directions. The heat energy generated from the kinetic energy increases the temperature of the flow. This is shown in figure 4.3 where temperature profile increases with increasing inclination angle. The maximum temperature profile is obtained at an inclination angle $\frac{\pi}{2}$. Figures (4.5) – (4.8) depict the variation of velocities, temperature and concentration with increasing porosity. Porosity ratio of empty spaces (or pores) to the volume of

the plate. Increasing porosity has a consequence of increasing viscosity of the fluid which in turn reduces the flow velocities. This is shown in Figures (4.5) and (4.6) where velocities decrease with porosity. Increasing porosity allows settlement of molecules at the wall of the plate and causes a surge in the concentration at the wall. Figure (4.7) shows the increase in the concentration at the wall as porosity increases. Transfer of heat from the wall to the free stream is slow and thereby enhances temperature profile. Thus, increasing porosity enhances temperature profile (Figure 4.8). Figures (4.9) – (4.12) show the effects of increasing MF on the flow properties. With magnetic field, the Lorentz force is generated. The Lorentz force resists motion and thereby reduces primary and secondary velocity. Hence, Figures (4.9) and (4.10) show that increasing MF strength causes a decrease in the flow velocities. Also, the resistance offered by Lorentz force generates more heat and thereby increases the flow temperature (see Figure (4.11) for the variation of temperature with MF parameter). Figure (4.12) shows that concentration increases with increasing MF strength.

Table 4.1 shows the variation of coefficient of skin friction with increasing magnetic field, porosity and inclination angle. The table shows that the skin friction increases with increasing magnetic field, porosity and inclination angle. Increase in the MF strength increases the viscous boundary layer and thereby raising the skin friction. The increase in the porosity enhances the migration of the fluid particles towards the boundary layer and thereby gives rise to an increase in the coefficient of skin friction. Also, as the angle of inclination increases from 0^o through 90^o, fluid particles are more attracted to the boundary layer. Hence, the skin friction is boosted as inclination angle increases.

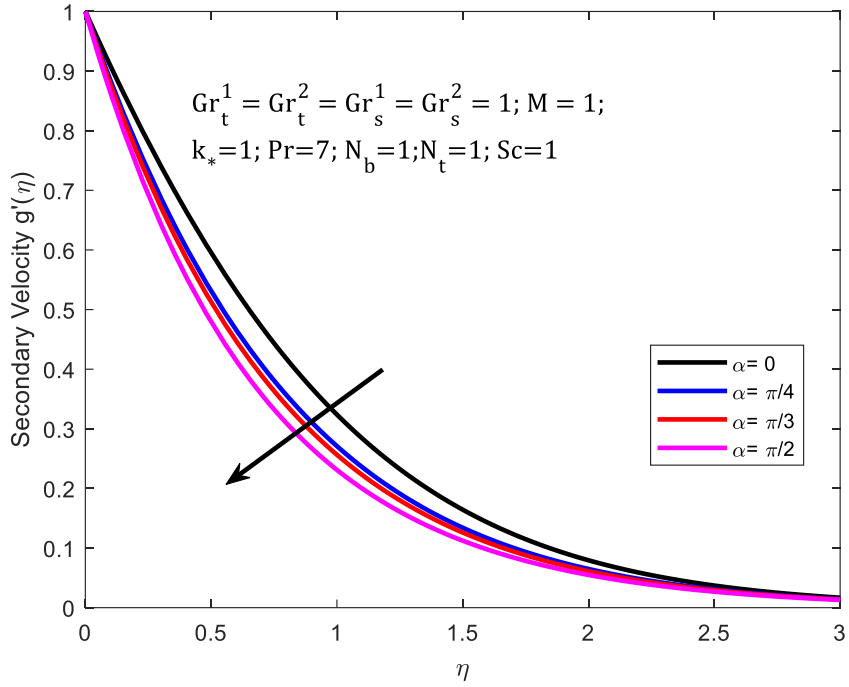

Figure 4.1: *Secondary velocity profile as inclination angle varies*

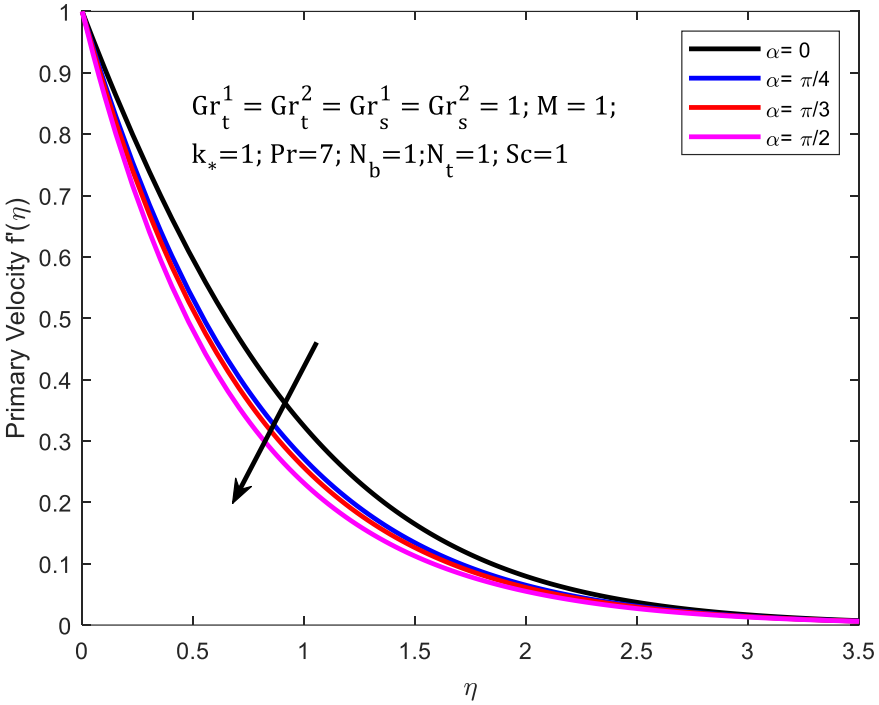

Figure 4.2: *Primary velocity profile as inclination angle varies*

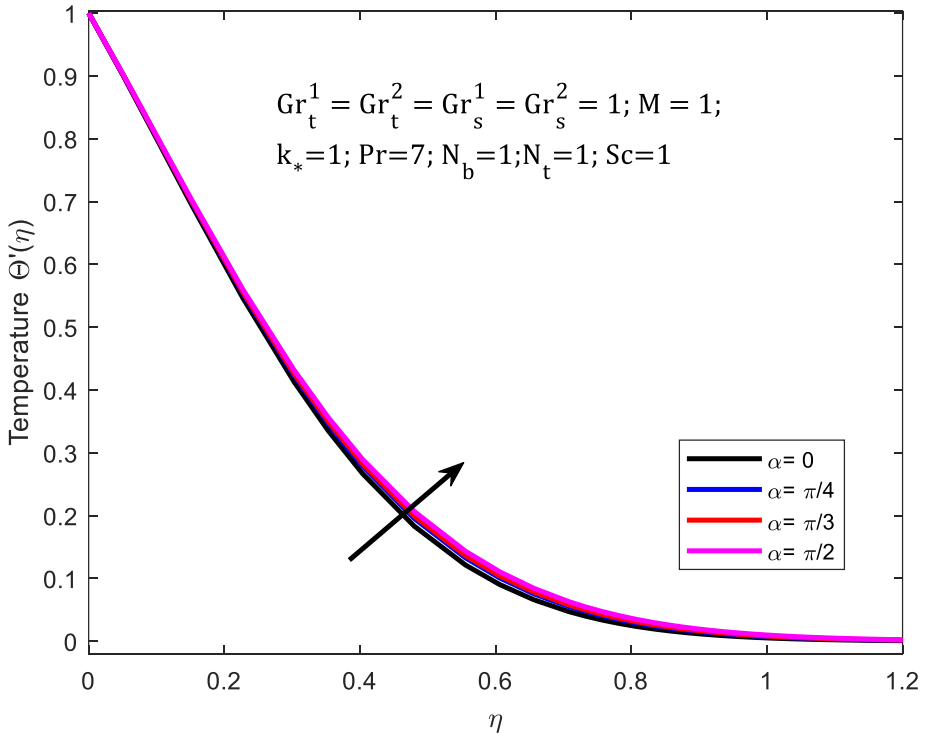

Figure 4.3: *Temperature profile as inclination angle varies*

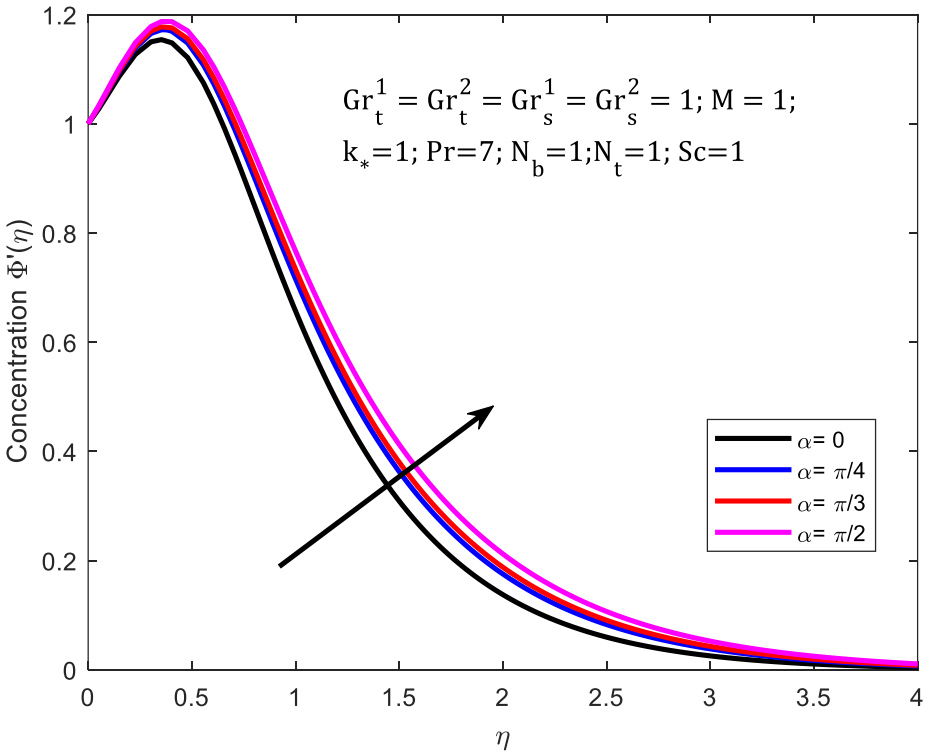

Figure 4.4: Concentration profile as inclination angle varies

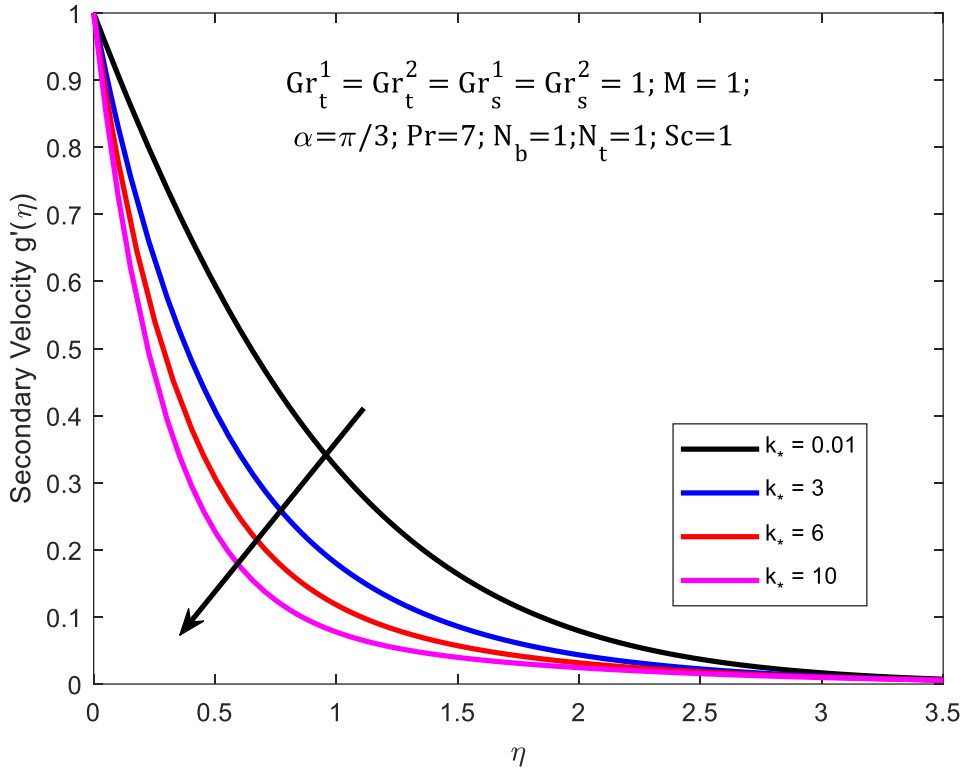

Figure 4.5: *Secondary velocity profile as porosity varies*

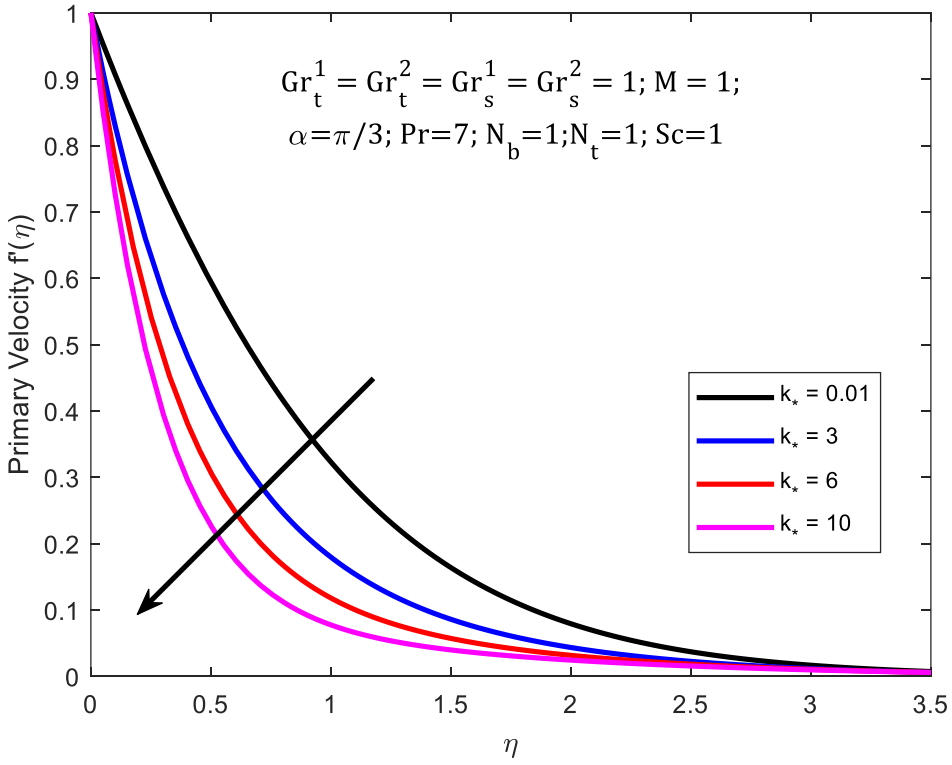

Figure 4.6: *Primary velocity profile as porosity varies*

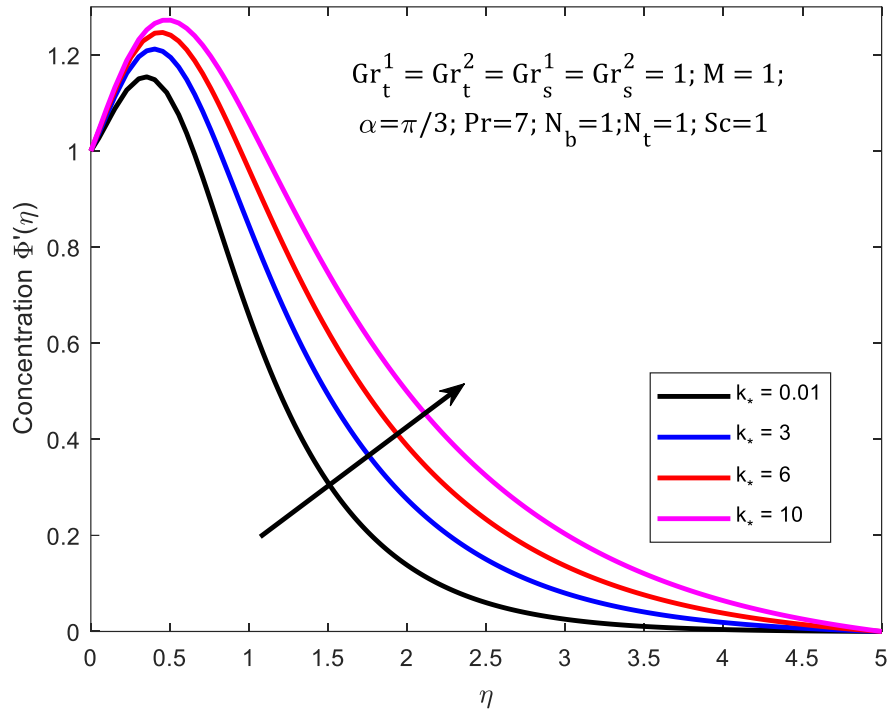

Figure 4.7: *Concentration profile as porosity varies*

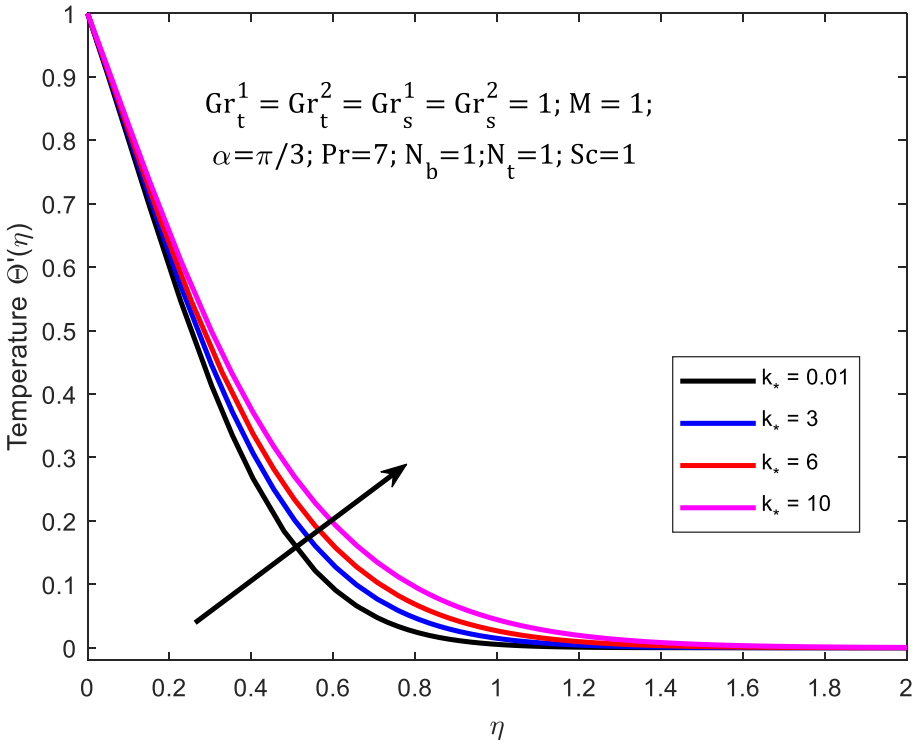

Figure 4.8: *Temperature profile as porosity varies*

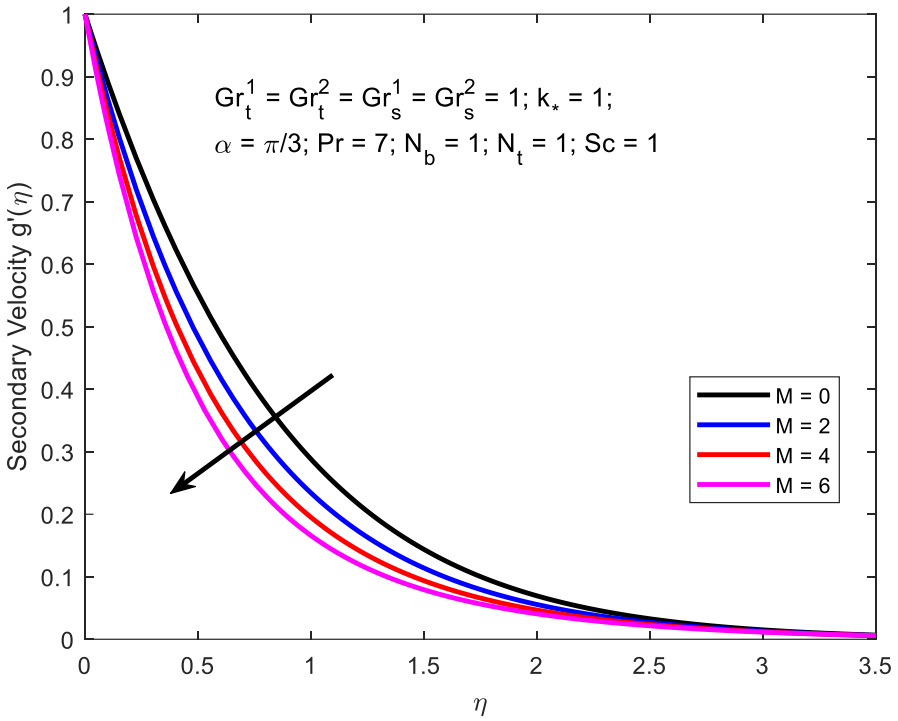

Figure 4.9: *Secondary velocity profile as MF parameter varies*

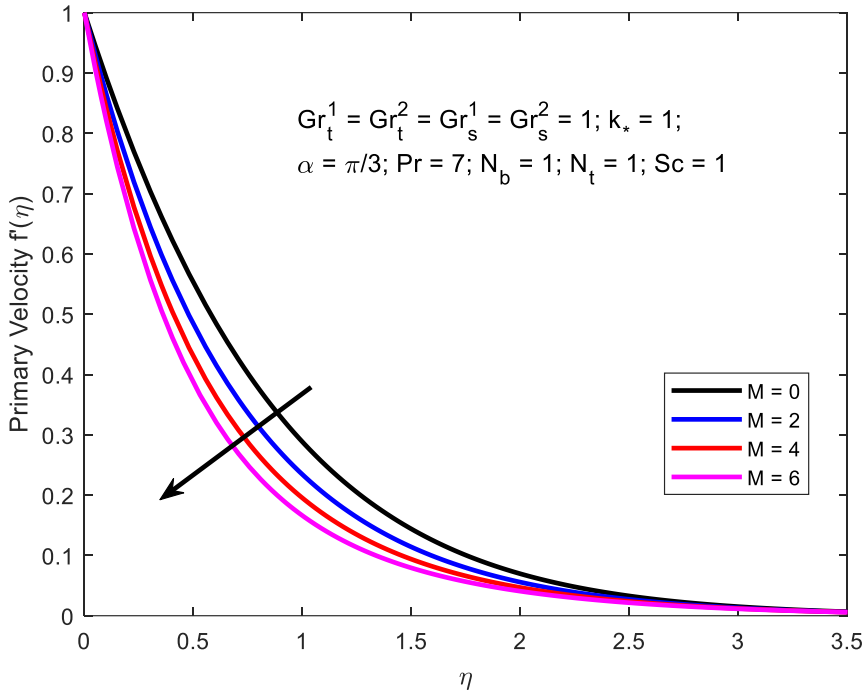

Figure 4.10: *Primary velocity profile as MF parameter varies*

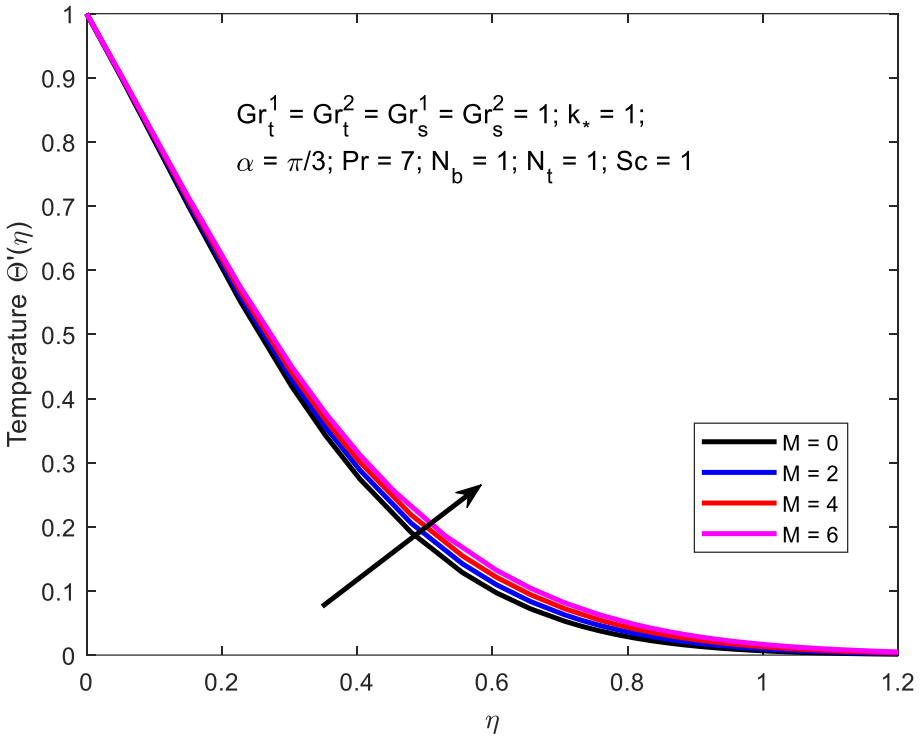

Figure 4.11: *Temperature profile as MF parameter varies*

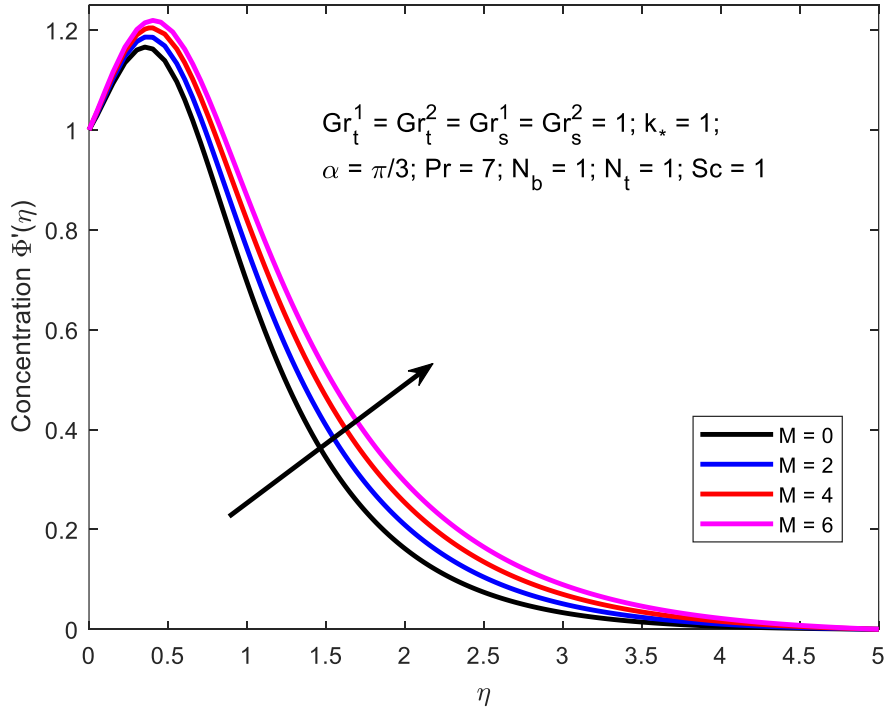

Figure 4.12: *Concentration profile as MF parameter varies*

M	k_*	α	|Skin Friction|
0.00	1.00	60^o	1.1233
1.00			1.2897
2.00			1.4434
3.00			1.5865
4.00			1.7208
5.00			1.8476
1.00	0.30		1.0525
	0.90		1.2575
	1.20		1.3525
	1.50		1.4434
	1.00	0^o	1.0916
		30^o	1.1417
		45^o	1.2037
		90^o	1.5357

Table 4.1: *Variation of coefficient of Skin Friction with magnetic field, porosity and inclination angle*

CHAPTER 5

Conclusion

The heat and mass transfer of the magnetohydrodynamics flow of a fluid across an inclined porous plate is modelled in this study. The governing equations comes out as a system of nonlinear PDEs. Similarity variables are used to transform the PDEs into a system of ODEs which are later solved using the Finite Difference method. The effects of inclination angle and porosity on the flow about an inclined porous plate are analysed and discussed. Increasing inclination angles reduces both the secondary velocity and the primary velocity and increases skin friction, temperature and concentration. The maximum temperature profile is obtained at an inclination angle $\frac{\pi}{2}$. Increasing porosity reduces both primary and secondary velocities but increases the concentration, skin friction and temperature at the wall. Raising the strength of the MF reduces primary and secondary velocity and increases the flow temperature. Also, Skin friction rises with magnetic field

REFERENCES

Ali, M. M., Mamun, A. A., Maleque, M. A., & Azim, N. H. M. A. (2013). Radiation effects on MHD free convection flow along vertical flat plate in presence of Joule heating and heat generation. *Procedia Engineering*, *56*, 503-509.

Animasaun, I. L., Oke, A. S., Al-Mdallal, Q. M., & Zidan, A. M. (2023). Exploration of water conveying carbon nanotubes, graphene, and copper nanoparticles on impermeable stagnant and moveable walls experiencing variable temperature: thermal analysis. Journal of Thermal Analysis and Calorimetry, 1-10.

Hamad, M. A. A., Pop, I., & Ismail, A. M. (2011). Magnetic field effects on free convection flow of a nanofluid past a vertical semi-infinite flat plate. *Nonlinear Analysis: Real World Applications*, *12*(3), 1338-1346.

Hayat T., Khan M.I., Tamoor M., Waqas M. and Alsaedi A., (2017). Numerical Simulation of Heat Transfer in MHD Stagnation Point Flow Of Cross Fluid Model Towards A Stretched Surface. *Results in Physics*, **7**, 1824-1827.

Juma, B. A., Oke, A. S., Mutuku, W. N., Ariwayo, A. G., & Ouru, O. J. (2022a). Dynamics of Williamson fluid over an inclined surface subject to Coriolis and Lorentz forces. Eng. Appl. Sci. Lett, 5(1), 37-46.

Juma, B. A., Oke, A. S., Ariwayo, A. G., & Ouru, O. J. (2022b). Theoretical Analysis of MHD Williamson Flow Across a Rotating Inclined Surface. *Applied Mathematics and Computational Intelligence (AMCI)*, *11*(1), 133-145.

Katagiri, Khan I., Fakhar K. and Shafie S., (2011). Magnetohydrodynamic Free Convection Flow Past An Oscillating Plate Embedded In A Porous Medium. *Journal Of the Physical Society Of Japan*, **80**(10), 104401.

Kọríkọ, O. K., Adegbie, K. S., Oke, A. S., & Animasaun, I. L. (2020a). Exploration of Coriolis force on motion of air over the upper horizontal surface of a paraboloid of revolution. *Physica Scripta*, *95*(3), 035210.

Koriko, O. K., Adegbie, K. S., Oke, A. S., & Animasaun, I. L. (2020b). Corrigendum: Exploration of Coriolis force on motion of air over the upper horizontal surface of a paraboloid of revolution.(2020 Phys. Scr. 95 035210). *Physica Scripta*, *95*(11), 119501.

Makinde O. D., Khan W. A. and Khan Z. H., (2014). Buoyancy effects On MHD Stagnation Point Flow and Heat Transfer of A nanofluid Past A convectively Heated Stretching/Shrinking Sheet. *International Journal of Heat And Mass Transfer*, **62**(1), 526-533.

Mbugua Z. M., (2016). Hydromagnetic Fluid Flow Between Parallel Plates Where The Upper Plate Is Porous In Presence Of Variable Transverse Magnetic Fields

Nyabuto R., Sigey K. J., (2015). Investigating The Unsteady MHD Mixed Convective Flow With Hall Effect Of A Viscous Incompressible Fluid Past A Vertical Porous Plate With Heat Source, *International Journal Of engineering Science And Innovative technology*, **7**(2): 52-62.

O. Anwar Bég, A.Y. Bakier, V.R. Prasad, (2009). Numerical study of free convection magnetohydrodynamic heat and mass transfer from a stretching surface to a saturated porous medium with Soret and Dufour effects, *Computational Materials Science*, 46(1) Pages 57-65, https://doi.org/10.1016/j.commatsci.2009.02.004.

Oke, A. S., Mutuku, W. N., Kimathi, M., & Animasaun, I. L. (2020). Insight into the dynamics of non-Newtonian Casson fluid over a rotating non-uniform surface subject to Coriolis force. Nonlinear Engineering, 9(1), 398-411.

Oke, A. S., Prasannakumara, B. C., Mutuku, W. N., Gowda, R. P., Juma, B. A., Kumar, R. N., & Bada, O. I. (2022). Exploration of the effects of Coriolis force and thermal radiation on water-based hybrid nanofluid flow over an exponentially stretching plate. Scientific Reports, 12(1), 21733.

Onyango E. R., Kinyanjui M. N.,and Uppal S. M., (2015). Analysis Of Unsteady Hydromagnetic Couette Flow with Magnetic Field Lines Fixed Relative to the Moving Upper Plate, *American Journal Of Applied Mathematics*, **3**(5), 206-214.

Ostrach Soundalgekar, (1972). Viscous Dissipation Effects on Unsteady Free Convective Flow Past An Infinite, Vertical Porous Plate With Constant Suction, *International Journal Of Heat And Mass Transfer* **15** (6), 1253-1261.

Rao A.J., Shivaiah S.,(2012). Chemical reaction effect on an unsteady MHD Free Convection Flow Past A Vertical Porous Plate In The Presence Of Suction Or Injection.

Reddy R.G.V. and Murthy C.V.R., (2011). MHD Flow Over A Vertical Moving Porous Plate With Heat Generation By Considering Double Diffusive Convection, *International Journal Of Applied Mathematics and Mechanics*, **7**(1), 1-17.

Singh L.P., Dash G.C. and Nayak M.K., (2015). Unsteady Radiative MHD Free Convective Flow and Mass Transfer Of a Viscoelastic Fluid Past An Inclined Porous Plate. *Arabian Journal For Science And Engineering*, **40**, 3029-3039.

Sundarammal K., and Nisha, (2019). Squeeze Film Characteristics Of MHNN Lubrication Of Porous Curved Circular Plates, *ARPN Journal Of Engineering And Applied Sciences,* **2112** (1), 020066

Umamaheswar M., Varma S.V.K., Raju M.C. and Chamkha A.J., (2016). Unsteady Magnetohydrodynamic Free Convective Double-Diffusive Viscoelastic Fluid Flow Past An Inclined Permeable Plate In The Presence Of Viscous Dissipation And Heat Absorption, *Special Topics & Reviews in Porous Media: An International Journal*, **6**(4)

Xing J. T. Chapter 3 - fundamentals of continuum mechanics. In Jing Tang Xing, editor, Fluid-Solid Interaction Dynamics, pages 57–101. Academic Press, 2019.